Sun-Avoidance Slew Planning Algorithm with Pointing and Actuator Constraints (AAS 19-801)

AIAA/AAS Astrodynamics Specialist Conference,
Portland, ME, 11– 15 August 2019

Mohammad. A. Ayoubi[1] Junette Hsin[2]

[1]Associate Professor, Department of Mechanical Engineering, Santa Clara University,
[2]Engineer, Dynamics and Control Analysis Group, Maxar Space Infrastructure
(Formerly Space Systems/Loral)

Outlines

Introduction

The attitude reorientation problem in the presence of attitude constrained zones has been studied in the last three decades:

1. McInnes (1994): artificial potential function. He proposed an entirely analytical guidance law which was suitable for onboard implementation.
   1. However, he used Euler angles, which are singular for large slew angles.
2. Spindle (1998), Hablani (1998), Biggs and Colley (2016), Frazzoli (2001): A geometric approach was proposed where a feasible attitude maneuver, or a guidance law, is precomputed based on the attitude-avoidance-zone constraints or randomized algorithms.
   1. However, depending on the number of constraints and initial and final attitudes, this approach can be computationally expensive and not suitable for onboard implementation.

Previous Literature

1. Spiller (2016): Particle swarm optimization (PSO) technique to find a sub-optimal solution with keep-out constraints.
2. Another approach casted the problem as a convex optimization problem and used semi-definite programming (SDP) or quadratically constrained quadratic programming (QCQP) in its solution (see for instance Kim and Mesbahi, Kim et al., Sun and Dai, and Lee and Mesbahi.
3. Recently, Ramos and Schaub proposed a method based on the Lyapunov stability theorem and logarithmic barrier potential function to derive a steering law for attitude control of a spacecraft subject to conically constrained inclusion and exclusion regions. They also considered the control-torque constraint in their algorithm.

SAS Algorithm

1. The SAS algorithm is a geometric approach for a sun (or any bright object) avoidance slew maneuver with pointing and actuator constraints.
2. Assumption: spacecraft has a single light-sensitive payload with control-torque and reaction wheels' angular momentum constraints
3. Assumption: The initial and final attitudes, instrument boresight vector, and sun vector are known.
4. Pontryagin's minimum principle (PMP) is used to derive the desired or target-frame quaternions, angular velocity and acceleration for two cases:
    1. with control-torque and reaction wheels' angular momentum constraints
    2. with control-torque constraints
5. Numerical simulation is performed to show the viability of the proposed algorithm with control-torque and angular momentum constraints.

Sun-Avoidance Slew (SAS) Algorithm

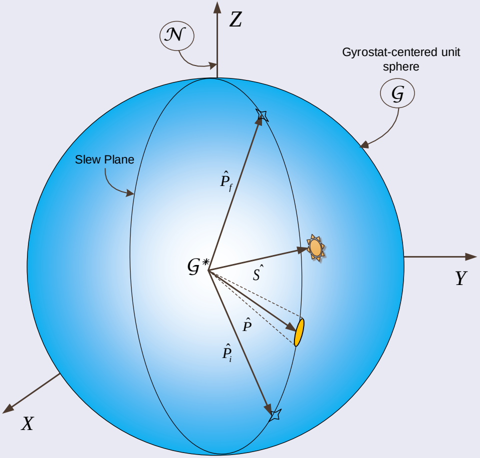

Figure: The gyrostat-centered unit sphere.

Sun-Avoidance Slew (SAS) Algorithm

Problem Statement:

Given: ${}_{\mathcal{N}}\hat{P}_i$, ${}_{\mathcal{N}}\hat{P}_f$, ${}_{\mathcal{N}}\hat{S}$, ${}_{\mathcal{G}}\hat{P}$, ϵ_p, ${}^{\mathcal{N}}q^{\mathcal{G}}$, ${}^{\mathcal{N}}_{\mathcal{G}}\omega^{\mathcal{G}}(t_i)$, and ${}^{\mathcal{N}}_{\mathcal{G}}\omega^{\mathcal{G}}(t_f)$.
Assumption: The spacecraft is rigid.
Find:

1. A sequence of slew maneuvers to avoid sun vector.
2. the commanded angular velocity, angular acceleration, and quaternion profiles.

Summary of the Algorithm

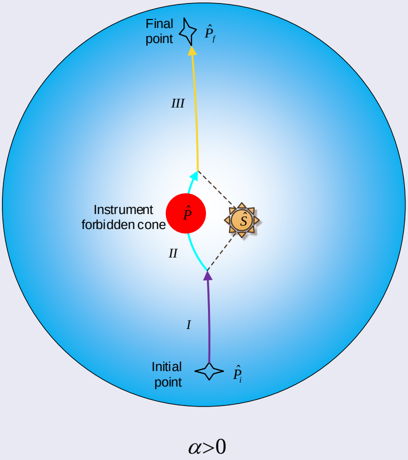

Sun-Avoidance Slew (SAS) Algorithm

Check the Sun Vector Intrusion

1. Check the angular separation, α, between the sun vector, $\hat{S}$, and the $\hat{P}_i - \hat{P}_f$ or "slew" plane.

$$\alpha = \frac{\pi}{2} - \cos^{-1}(\hat{S} \cdot_{\mathcal{N}} \hat{e}) \tag{1}$$

   where the eigenaxis is determined by

$$\hat{e} = \frac{\hat{P}_i \times \hat{P}_f}{|\hat{P}_i \times \hat{P}_f|} \tag{2}$$

2. IF $|\alpha| < \epsilon_p$,THEN determine the projection of the sun vector into the slew plane.

$$\vec{S}_{||} = \hat{S} \cos \alpha \tag{3}$$

Sun-Avoidance Slew (SAS) Algorithm

Slew Maneuvers

1. The 1^{st} slew around the eigenaxis, $\hat{e}$, through angle:

$$\phi_1 = \begin{cases} \cos^{-1}(\hat{P}_i \cdot_G \hat{S}_{||}) - \epsilon_p & \text{when } \cos^{-1}(\hat{P}_i \cdot_G \hat{S}_{||}) - \epsilon_p \leq \pi \\ \cos^{-1}(\hat{P}_i \cdot_G \hat{S}_{||}) - \epsilon_p - 2\pi & \text{when } \cos^{-1}(\hat{P}_i \cdot_G \hat{S}_{||}) - \epsilon_p > \pi \end{cases} \quad (4)$$

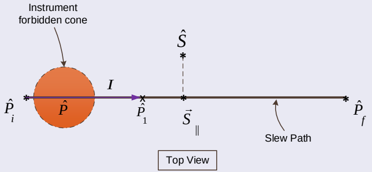

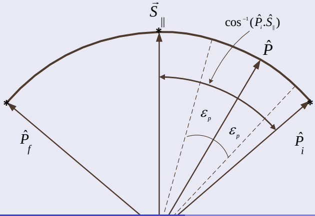

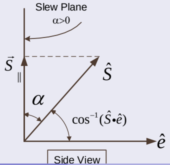

Sun-Avoidance Slew (SAS) Algorithm

Slew Maneuvers

2. The 2^{nd} slew around the unit sun vector, $\hat{S}$, via ϕ_2.
   a. when $\alpha \neq 0$

$$\phi_2 = 2\tan^{-1}\left[\frac{\hat{S}\cdot(\hat{P}_1\times\hat{S}_{||})}{(\hat{P}_1\cdot\hat{S}_{||})-(\hat{S}\cdot\hat{P}_1)(\hat{S}\cdot\hat{S}_{||})}\right], \qquad (5)$$

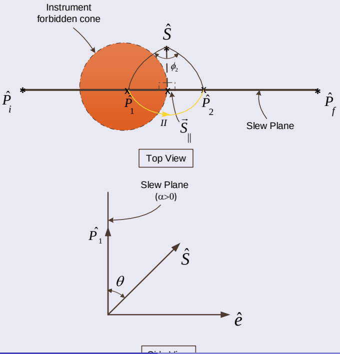

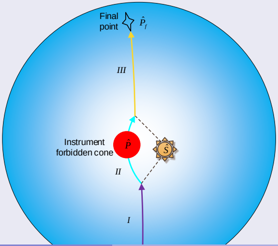

Sun-Avoidance Slew (SAS) Algorithm

Slew Maneuvers

2. The 2^{nd} slew around the unit sun vector, $\hat{S}$, via $\phi_2 = 180°$.
   b) when $\alpha = 0$

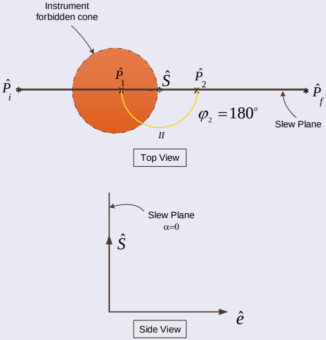

Sun-Avoidance Slew (SAS) Algorithm

Slew Maneuvers

3. The 3^{rd} slew about the $\hat{e}$ through angle:

$$\phi_3 = \begin{cases} \cos^{-1}({}_G\hat{P}_f.\hat{P}_2) & when\ {}_G\hat{P}_f.\hat{P}_2 \geq 0 \\ \cos^{-1}({}_G\hat{P}_f.\hat{P}_2) - 2\pi & when\ {}_G\hat{P}_f.\hat{P}_2 < 0 \end{cases} \quad (6)$$

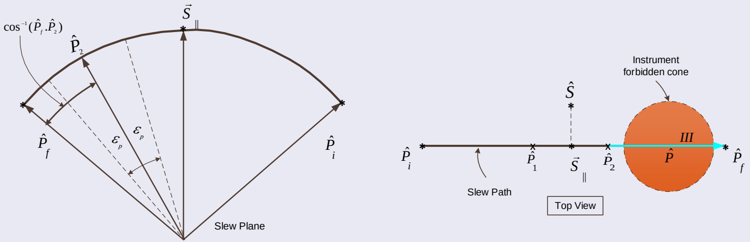

4. The final slew is about the instrument boresight axis to go to the final attitude.

Summary of the Algorithm

1. Slew around the eigenaxis, $\hat{e}$, through angle:

$$\phi_1 = \begin{cases} \cos^{-1}(\hat{P}_i \cdot_{\mathcal{G}} \hat{S}_{||}) - \epsilon_p & \textit{when } \cos^{-1}(\hat{P}_i \cdot_{\mathcal{G}} \hat{S}_{||}) - \epsilon_p \leq \pi \\ \cos^{-1}(\hat{P}_i \cdot_{\mathcal{G}} \hat{S}_{||}) - \epsilon_p - 2\pi & \textit{when } \cos^{-1}(\hat{P}_i \cdot_{\mathcal{G}} \hat{S}_{||}) - \epsilon_p > \pi \end{cases} \tag{7}$$

2. Slew around the $\hat{S}$ via:

$$\phi_2 = \begin{cases} \phi_2 = 2\tan^{-1}\left[\frac{\hat{S}\cdot(\hat{P}_1 \times \hat{S}_{||})}{(\hat{P}_1\cdot\hat{S}_{||}) - (\hat{S}\cdot\hat{P}_1)(\hat{S}\cdot\hat{S}_{||})}\right], & \textit{when } \alpha \neq 0 \\ \pi & \textit{when } \alpha = 0 \end{cases} \tag{8}$$

3. Slew about the $\hat{e}$ through angle:

$$\phi_3 = \begin{cases} \cos^{-1}({}_{\mathcal{G}}\hat{P}_f.\hat{P}_2) & \textit{when } {}_{\mathcal{G}}\hat{P}_f.\hat{P}_2 \geq 0 \\ \cos^{-1}({}_{\mathcal{G}}\hat{P}_f.\hat{P}_2) - 2\pi & \textit{when } {}_{\mathcal{G}}\hat{P}_f.\hat{P}_2 < 0 \end{cases} \tag{9}$$

Computing the Steering Profiles

Single-Axis, Agile Slew Maneuver with Velocity and Acceleration Constraints.

Computing Steering Profiles

Problem Statement

Consider the motion of a rigid spacecraft around a given inertially-fixed axis, ${}_{G}\hat{e} = [e_x, e_y, e_z]^T$. The problem of minimum-time slew maneuver around the $\hat{e}$ axis can be formulated as

$$\underset{u}{Minimze}\; J[x(.), u(.), t_f] = \int_{t0}^{t_f} dt, \tag{10}$$

subject to the following dynamic constraint

$$\Sigma : \begin{cases} \dot{x}_1 = x_2, \\ \dot{x}_2 = M/I_{\hat{e}}^{G/G*} = u, \end{cases} \tag{11}$$

where $x_1 \triangleq \phi$ and $x_2 = \dot{\phi}$.

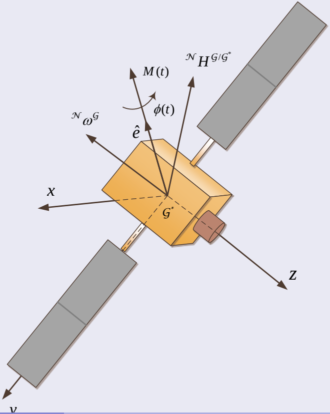

Computing Steering Profiles

Problem Statement Continued

The boundary conditions are

$$BCs : \begin{cases} \phi(t_0) = 0, \phi(t_f) = \phi_f, \\ \dot{\phi}(t_0) = \dot{\phi}_0, \dot{\phi}(t_f) = \dot{\phi}_f, \end{cases} \tag{12}$$

and velocity (state) and acceleration (control) constraints are

$$C_1 : \begin{cases} |x_2 = \dot{\phi}| \leq \dot{\phi}_{max}, \\ |u = \ddot{\phi}| \leq \ddot{\phi}_{max}, \end{cases} \tag{13}$$

Find: $\phi(t)$, $\dot{\phi}(t)$, and $\ddot{\phi}(t)$.

Computing Steering Profiles

- Angular acceleration profile (bang-off-bang):

$$\ddot{\phi}(t) = u = \begin{cases} \ddot{\phi}_{max} & \text{when } t_0 \le t \le t_1, \\ 0 & \text{when } t_1 \le t \le t_2, \\ -\ddot{\phi}_{max} & \text{when } t_2 \le t \le t_f. \end{cases} \tag{14}$$

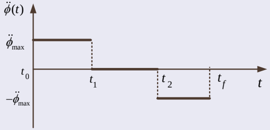

- Angular velocity profile:

$$\dot{\phi}(t) = \begin{cases} \dot{\phi}_0 + \ddot{\phi}_{max}(t - t_0) & \text{when } t_0 \le t \le t_1, \\ \dot{\phi}_{max} & \text{when } t_1 \le t \le t_2, \\ \dot{\phi}_{max} - \ddot{\phi}_{max}(t - t_2) & \text{when } t_2 \le t \le t_f. \end{cases} \tag{15}$$

- Angular position profile:

$$\phi(t) = \begin{cases} \dot{\phi}_0(t - t_0) + \frac{1}{2}\ddot{\phi}_{max}(t - t_0)^2 & \text{when } t_0 \le t \le t_1, \\ \phi(t_1) + \dot{\phi}_{max}(t - t_1) & \text{when } t_1 \le t \le t_2, \\ \phi(t_2) + \dot{\phi}_{max}(t - t_2) - \frac{1}{2}\ddot{\phi}_{max}(t - t_2)^2 & \text{when } t_2 \le t \le t_f. \end{cases} \tag{16}$$

Computing Steering Profiles

- Using the conditions, $\dot{\phi}(t_1) = \dot{\phi}_{max}$, $\dot{\phi}(t_f) = \dot{\phi}_f$, $\phi(t_f) = \phi_f$, we can determine switching times t_1, t_2, and final time t_f as:

$$t_1 = t_0 + \frac{\dot{\phi}_{max} - \dot{\phi}_0}{\ddot{\phi}_{max}}, \tag{17}$$

$$\begin{aligned} t_2 = & t_1 + \frac{1}{\dot{\phi}_{max}} \left[\phi_f - \dot{\phi}_0(t_1 - t_0) - \frac{1}{2}\ddot{\phi}_{max}(t_1 - t_0)^2 \right. \\ & \left. - \frac{\dot{\phi}_{max}(\dot{\phi}_{max} - \dot{\phi}_f)}{\ddot{\phi}_{max}} + \frac{(\dot{\phi}_{max} - \dot{\phi}_f)^2}{2\ddot{\phi}_{max}} \right], \end{aligned} \tag{18}$$

and

$$t_f = t_1 + \frac{1}{\dot{\phi}_{max}} \left[\phi_f - \dot{\phi}_0(t_1 - t_0) - \frac{1}{2}\ddot{\phi}_{max}(t_1 - t_0)^2 + \frac{(\dot{\phi}_{max} - \dot{\phi}_f)^2}{2\ddot{\phi}_{max}} \right]. \tag{19}$$

Computing Steering Profiles

- Steering profiles:

$$^{N}q^{D}(t) = [e_x \sin\frac{\phi(t)}{2}, e_y \sin\frac{\phi(t)}{2}, e_z \sin\frac{\phi(t)}{2}, \cos\frac{\phi(t)}{2}]^T \tag{20}$$

$$^{N}_{G}\omega^{D}(t) = \dot{\phi}(t)_G\hat{e} \tag{21}$$

$$^{N}_{G}\alpha^{D}(t) = \ddot{\phi}(t)_G\hat{e} \tag{22}$$

Numerical Simulations

Introduction

1. Matlab was used to numerically simulate and examine the proposed algorithm.
2. The initial, final, and sun position vectors were randomized for each run.
3. Two cases shown in these slides - one in which the sun angle is greater than 0 from the slew plane, the other in which the sun vector lies directly on the slew plane.
4. Slew angles were found using the methods discussed in the description of the algorithm.

Numerical Simulations

$\alpha > 0$

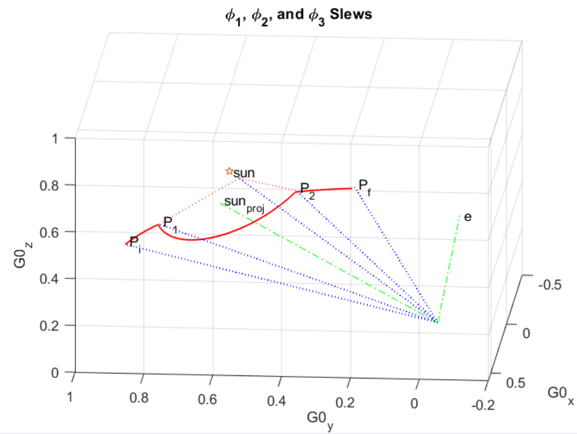

Figure: Attitude Profile of the Entire Slew

Numerical Simulations

α¿0

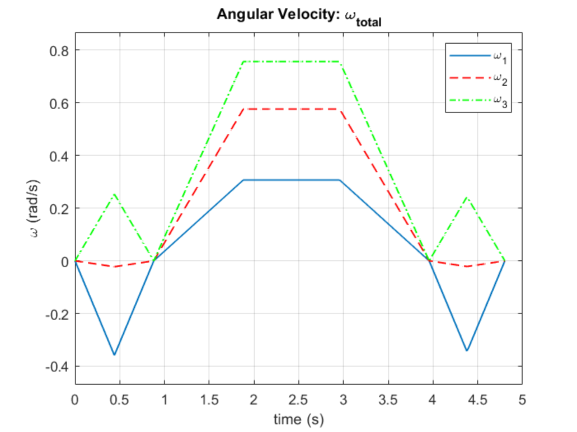

Figure: Angular Velocity in Spacecraft Frame

Numerical Simulations

$\alpha > 0$

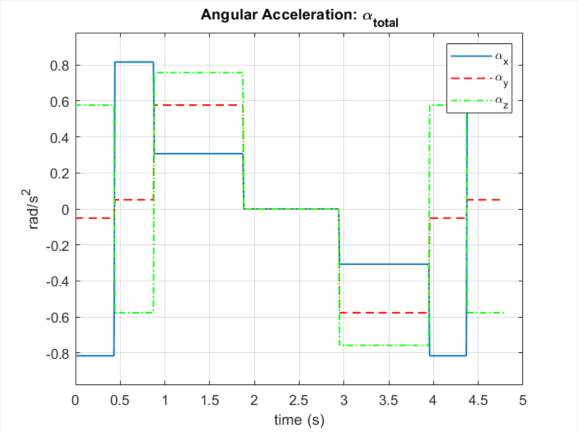

Figure: Angular Acceleration

Numerical Simulations

$\alpha > 0$

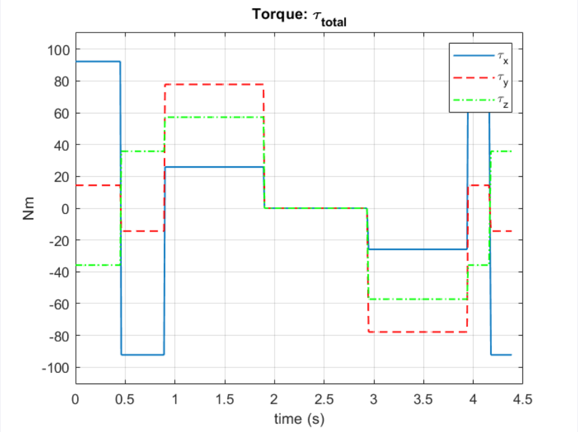

Figure: Torque Applied from Actuator System

Numerical Simulations

$\alpha > 0$

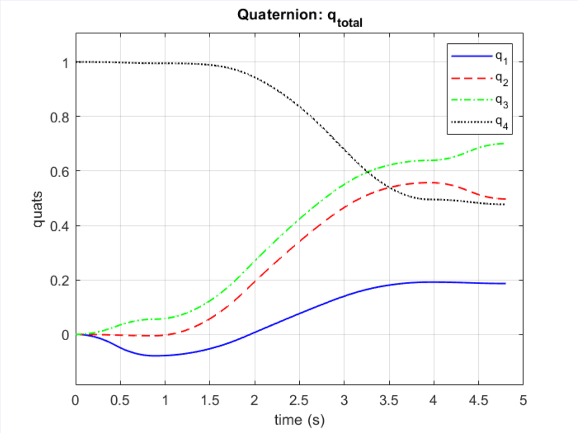

Figure: Quaternion Attitude

Summary and Conclusion

1. Geometric approach for large-angle slew planning with pointing and actuator constraints
2. Assumed that initial and final attitudes, instrument boresight, and sun vector are known
3. Target-frame quaternions, angular velocities, and angular accelerations are derived base on the PMP
4. Limitation is for single sensitive-payload

Acknowledgments

The research has been supported by Maxar Space Solutions (formerly Space Systems/Loral). The second author (Junette Hsin) would like to acknowledge Luke DeGalan for his useful comments.

Q & A

Back-up Slides

Computing the Steering Profiles

Case II: Single-Axis, Agile Slew Maneuver with Acceleration Constraint.

Single-Axis, Agile Slew Maneuver with Acceleration Constraint

Problem Statement:

Consider the optimal control problem described by Eqs.(10), (11), (12), and subject to control constraint

$$C_2 : \; |u = \ddot{\phi}| \leq \ddot{\phi}_{max}. \tag{23}$$

Find: $\phi(t)$, $\dot{\phi}(t)$, and $\ddot{\phi}(t)$.

Single-Axis, Agile Slew Maneuver with Acceleration Constraint

- Angular acceleration about the $\hat{e}$ axis:

$$\ddot{\phi}(t) = \ddot{\phi}_{max}\mathbb{U}(t_0) - 2\ddot{\phi}_{max}\mathbb{U}(t - t_1) \tag{24}$$

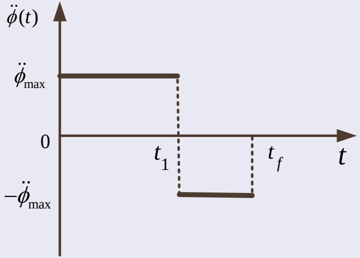

where the switching and the final times are given by

$$t_1 = t_0 - \frac{\dot{\phi}_0}{\ddot{\phi}_{max}} + \frac{\sqrt{\ddot{\phi}_{max}^2(2\ddot{\phi}_{max}\phi_f + \dot{\phi}_f^2 + \dot{\phi}_0^2)}}{\sqrt{2}\ddot{\phi}_{max}^2} \tag{25}$$

Single-Axis, Agile Slew Maneuver with Acceleration Constraint

and

$$t_f = t_0 - \frac{\dot{\phi}_f + \dot{\phi}_0}{\ddot{\phi}_{max}} + \frac{\sqrt{2}\sqrt{\ddot{\phi}_{max}^2(2\ddot{\phi}_{max}\phi_f + \dot{\phi}_{ef}^2 + \dot{\phi}_0^2)}}{\ddot{\phi}_{max}^2} \tag{26}$$

- Angular velocity about the $\hat{e}$ axis:

$$\dot{\phi}(t) = \dot{\phi}_0 + \ddot{\phi}_{max}(t - t_0)\mathbb{U}(t_0) - 2\ddot{\phi}_{max}(t - t_1)\mathbb{U}(t - t_1) \tag{27}$$

- Angular position about the $\hat{e}$ axis:

$$\begin{aligned} \phi(t) = {} & \dot{\phi}_0(t - t_0) + \ddot{\phi}_{max}\frac{(t - t_0)^2}{2}\mathbb{U}(t_0) \\ & - 2\ddot{\phi}_{max}\frac{(t - t_1)^2}{2}\mathbb{U}(t - t_1) \end{aligned} \tag{28}$$

The Agile Sun-Avoidance Slew Maneuver

The First Slew Maneuver:
A single-axis nonrest-to-rest maneuver around the ê

- The BCs:

$$\dot{\phi}(t_0) = \dot{\phi}_0, \phi(t_0) = 0, \dot{\phi}(t_{f1}) = 0, \phi(t_{f1}) = \phi_1. \tag{29}$$

The switching time, t_{11}, and minimum-time, t_{f1}, are

$$t_{11} = t_0 - \frac{\dot{\phi}_0}{\ddot{\phi}_{max}} + \frac{\sqrt{\ddot{\phi}^2_{max}(2\ddot{\phi}_{max}\phi_1 + \dot{\phi}^2_0)}}{\sqrt{2}\ddot{\phi}^2_{max}} \tag{30}$$

$$t_{f1} = t_0 - \frac{\dot{\phi}_0}{\ddot{\phi}_{max}} + \frac{\sqrt{2\ddot{\phi}^2_{max}(2\ddot{\phi}_{max}\phi_1 + \dot{\phi}^2_0)}}{\ddot{\phi}^2_{max}} \tag{31}$$

The $\ddot{\phi}(t)$, $\dot{\phi}(t)$, and $\phi(t)$, can be found by substituting the boundary conditions given by (29) and t_{11} and t_{f1} in to Eqs. (24), (27), and (28), respectively.

The Agile Sun-Avoidance Slew Maneuver

The Second Slew Maneuver: A rest-to-rest maneuver around the sun vector

- The BCs:

$$\dot{\phi}(t_0) = 0, \phi(t_0) = 0, \dot{\phi}(t_{f2}) = 0, \phi(t_{f2}) = \phi_2. \tag{32}$$

The switching time, t_{12}, and the minimum-time, t_{f2}, are

$$t_{12} = t_0 - \frac{\sqrt{\phi_2}}{\ddot{\phi}_{max}} \tag{33}$$

$$t_{f2} = t_0 - \frac{2\sqrt{\phi_2}}{\ddot{\phi}_{max}} \tag{34}$$

The $\ddot{\phi}(t)$, $\dot{\phi}(t)$, and $\phi(t)$, can be found by substituting the boundary conditions given by (32) and t_{12} and t_{f2} in to Eqs. (24), (27), and (28), respectively.

The Third Slew Maneuver: A single-axis rest-to-nonrest maneuver around the $\hat{e}$

- The BCs:

$$\dot{\phi}(t_0) = 0, \phi(t_0) = 0, \dot{\phi}(t_{f3}) = \dot{\phi}_f, \phi(t_{f3}) = \phi_3. \tag{35}$$

The switching time, t_{13}, and the minimum-time, t_{f3}, are

$$t_{13} = t_0 + \frac{\sqrt{\ddot{\phi}_{max}^2(2\ddot{\phi}_{max}\phi_3 + \dot{\phi}_f^2)}}{\sqrt{2}\ddot{\phi}_{max}^2} \tag{36}$$

$$t_{f3} = t_0 - \frac{\dot{\phi}_f}{\ddot{\phi}_{max}} + \frac{\sqrt{2\ddot{\phi}_{max}^2(2\ddot{\phi}_{max}\phi_3 + \dot{\phi}_f^2)}}{\ddot{\phi}_{max}^2} \tag{37}$$

The $\ddot{\phi}(t)$, $\dot{\phi}(t)$, and $\phi(t)$, can be found by substituting the boundary conditions given by (35) and t_{13} and t_{f3} in to Eqs. (24), (27), and (28), respectively.

Computing Steering Profiles

Using the Pontryagin's minimum principle (PMP), we derive the necessary conditions for the optimal solution as follows:

1. State Eqs.:

$$\begin{cases} \dot{x}_1 = x_2, \\ \dot{x}_2 = u, \\ \dot{x}_3 = (x_2 + \dot{\phi}_{max})^2 \mathbb{U}(-x_2 - \dot{\phi}_{max}) + (\dot{\phi}_{max} - x_2)^2 \mathbb{U}(x_2 - \dot{\phi}_{max}), \end{cases} \tag{38}$$

   where the unit step function, $\mathbb{U}$, is defined as

$$\mathbb{U}(X) = \begin{cases} 1, X > 0, \\ 0, X \leq 0. \end{cases} \tag{39}$$

   Note: $(x_3(t_0) = x_3(t_f) = 0 \;\&\; x_3(t) \geq 0\,) \rightarrow x_3(t) = 0, \forall t \in [t_0, t_f]$.

2. Hamiltonian:

$$\begin{aligned} \mathscr{H} =& 1 + \lambda_1 x_2 + \lambda_2 u + \lambda_3 \Big[(x_2 + \dot{\phi}_{max})^2 \mathbb{U}(-x_2 - \dot{\phi}_{max}) \\ & (\dot{\phi}_{max} - x_2)^2 \mathbb{U}(x_2 - \dot{\phi}_{max}) \Big] \end{aligned} \tag{40}$$

Computing Steering Profiles

3. Costate Eqs.:

$$\begin{cases} \dot{\lambda}_1 = -\frac{\partial \mathscr{H}}{\partial x_1} = 0, \\ \dot{\lambda}_2 = -\frac{\partial \mathscr{H}}{\partial x_2} = -\lambda_1 - 2\lambda_3(x_2 + \dot{\phi}_{max})\mathbb{U}(-x_2 - \dot{\phi}_{max}) \\ +2\lambda_3(\dot{\phi}_{max} - x_2)\mathbb{U}(x_2 - \dot{\phi}_{max}), \\ \dot{\lambda}_3 = -\frac{\partial \mathscr{H}}{\partial x_3} = 0. \end{cases} \tag{41}$$

4. Applying the Pontryagin's minimum principle (PMP),

$$u^* = \underset{u \in \mathcal{U}}{argmin} \mathscr{H}, \tag{42}$$

where $\mathcal{U}$ defines the domain of feasible controls. The optimal control can be determined as

$$u^*(t) = \begin{cases} \ddot{\phi}_{max} \lambda_2 < 0, \\ ? \lambda_2 = 0, \\ -\ddot{\phi}_{max} \lambda_2 > 0. \end{cases} \tag{43}$$

This is a *singular arc* optimal control problem.

Computing Steering Profiles

5. Determining the optimal control in the singular arc:

$$\frac{d^2}{dt^2}\left(\frac{\partial \mathscr{H}}{\partial u}\right) = \ddot{\lambda}_2 = 0 \rightarrow \dot{x}_2 = 0 \rightarrow u^* = 0 \tag{44}$$

6. Checking the Generalized Legendre-Clebsch condition for optimality:

$$(-1)^2 \frac{\partial}{\partial u}\left[\frac{d^2}{dt^2}\left(\frac{\partial \mathscr{H}}{\partial u}\right)\right] = 1 \geq 0 \tag{45}$$

7. The transversality condition:

$$\mathscr{H}|_{(*,t_f)} = 0 \text{ and } \mathscr{H} \neq \mathscr{H}(t) \rightarrow \mathscr{H} = 0, \forall t \in [t_0, t_f]. \tag{46}$$

Numerical Simulations

$\alpha = 0$

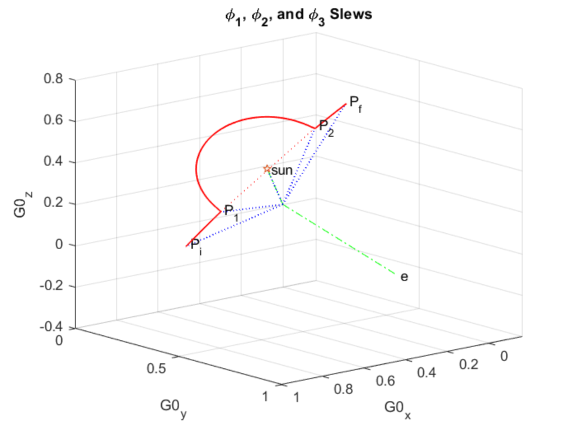

Figure: Attitude Profile of the Entire Slew

Numerical Simulations

$\alpha = 0$

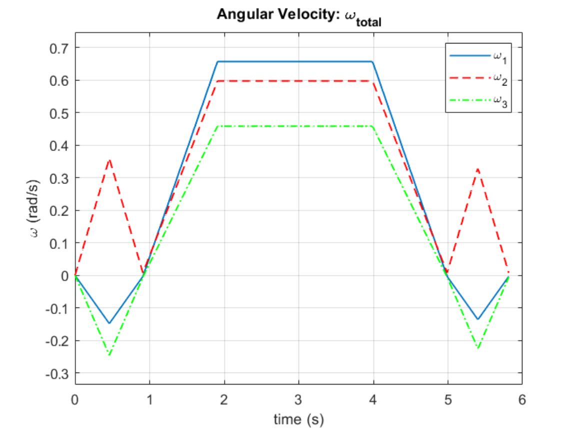

Figure: Angular Velocity in Spacecraft Frame

Numerical Simulations

$\alpha = 0$

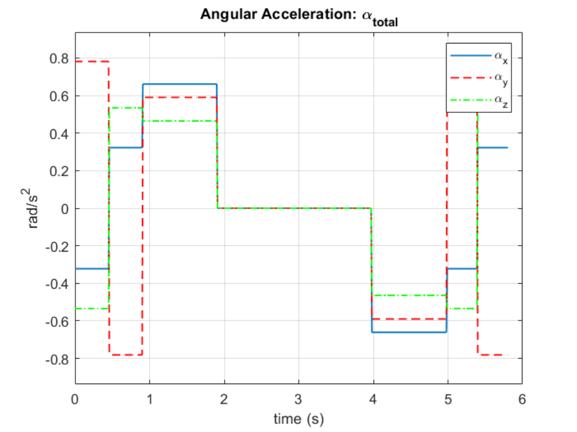

Figure: Angular Acceleration

Numerical Simulations

$\alpha = 0$

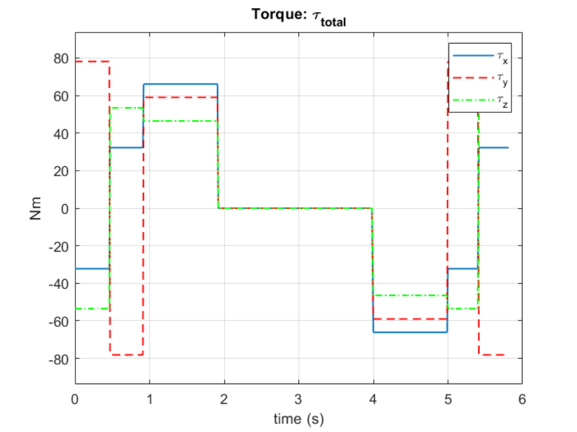

Figure: Torque Applied from Actuator System

Numerical Simulations

$\alpha = 0$

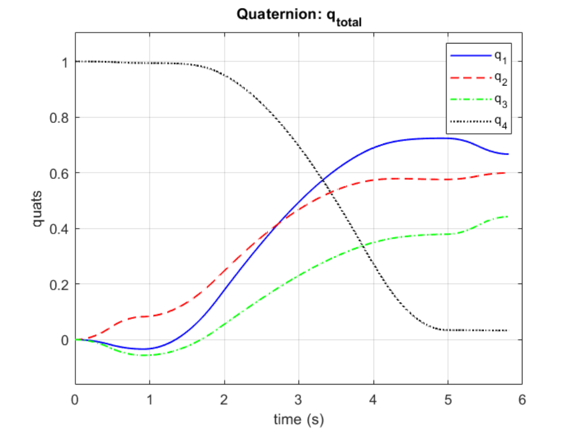

Figure: Quaternion Attitude